2022

Pathogenic mechanism of paclitaxel coated balloons and protective effects of dexameth

BOSTON UNIVERSITY

SCHOOL OF MEDICINE

Thesis

PATHOGENIC MECHANISM OF PACLITAXEL COATED BALLOONS AND PROTECTIVE EFFECTS OF DEXAMETHASONE

by

MENGWEI ZHANG

B.S., University of Waterloo, 2020

Submitted in partial fulfillment of the

requirements for the degree of

Master of Science

2022

Approved by

First Reader ____

Vipul Chitalia, M.D., Ph.D.
Renal Section
Associate Professor of Medicine

Second Reader ____

Christopher Andry, MPhil, PhD
Professor and Chair
Department of Pathology & Laboratory Medicine
Boston University School of Medicine

ACKNOWLEDGMENTS

I would like to acknowledge all those who have played a role in my academic accomplishments. Firstly, I would like to thank my family and friends for the endless support in my journey. I would not be able to achieve my current level of success and without any of you. Secondly, I am extremely grateful for Dr. V. Chitalia and the other members of his lab: X. Yang, S. Lotfollahzadeh, N. Elzinad, A. Morrissey, W. Yin, and M. Napoleon. Each of you played a vital role in the planning and development of this project and thesis. Thirdly, I would like to thank M, Elsadawi, M. Kirber, V. Kolachalama, A. Gower, E. Duffy, and C. Andry for the hard work, guidance, and teachings that all of you provided.

PATHOGENIC MECHANISM OF PACLITAXEL COATED BALLOONS AND PROTECTIVE EFFECTS OF DEXAMETHASONE

MENGWEI ZHANG

ABSTRACT

Cardiovascular disease (CVD) is the world's first leading cause of death contributing to 18.8 million global deaths worldwide. Lower extremity peripheral artery disease (PAD) stems from CVD and is the third leading cause of atherosclerotic morbidity. The prevalence of PAD increases significantly with age, and complications can lead to ischemia, non-healing wounds, gangrene, and amputation. Percutaneous transluminal angioplasty (PTA) and stenting are the mainstream techniques used to treat severe PAD. Due to high risk of restenosis within 12 months of the procedure, drug-coated balloons (DCB) and drug eluting-stents (DES) have become the standard of care since the early 2000s. Paclitaxel (PTX) is an extremely potent anti-restenotic agent used to coat balloons and stents to inhibit the assembly of microtubules, thereby inhibiting cell division. A recent systemic review and meta-analysis examined the all-cause of death rates at 1-year, 2-year, and 5-years of PCB and PES in the femoral and/or popliteal arteries versus control. The authors demonstrated a significantly increased risk of death in the PTX arm, which resulted in a warning from the FDA and a halt in the use of PTX devices. The massive release of PTX following balloon or stent application on the vessel wall and into systemic circulation may attribute to delayed systemic toxicity. Dexamethasone (DEX) is a glucocorticoid what may serve as an alternative anti-restenotic agent. In this study, we examined PTX induced toxicity in endothelial cells using cell biological assays and migration assay. This study

showed that PTX significantly reduced EC survival, proliferation, and migration. DEX was able to partially rescue the EC functions but was unable to abrogate PTX-induced inhibition of EC migration. RNA sequencing was used to examine differentially expressed genes modulated by PTX and DEX. Protein expression of MCP-1, CKS-2, CD137, and BMF were analyzed with western blots and found that DEX was able to abrogate the PTX induced effects. Overall, this study was the first to examine the potential mechanism(s) of PTX induced systemic toxicity in CVD and may serve as a stepping stone for future investigations to abrogate the adverse effects of PTX mediated devices.

TABLE OF CONTENTS

LIST OF TABLES

LIST OF FIGURES

LIST OF ABBREVIATIONS

ANOVA……………………………………………………………….Analysis of variance

BMS……………………………………………..………………………Bare metal stent

BMF..…………………………………………………………….Bcl2 modifying factor

CVD…………………………………………………………..….Cardiovascular disease

CKS-2………...……………………………….CDC28 protein kinase regulatory subunit-2

CLI……….……………………………………….………………Critical limb ischemia

CCR2………………………………….....…………….C-C chemokine receptor type 2

DEX…………………………..………………………………………….Dexamethasone

DCB……………………………….....…………………………….Drug-coated balloon

DES…………………………………...…………………………….Drug-eluting stent

EC………………………………………….………………………….Endothelial cell

FDR…………………………………………………………………False discovery rate

GSEA……………………………………………………...Gene set enrichment analysis

IC50………………………………….……….Half-maximal inhibitory concentration

HUVEC.…………………………………………Human umbilical cord endothelial cell

IL-1b……………………………….....……………………………Interleukin-1 beta

MMP……………………………...………………………..Matrix metalloproteinases

MCP-1…………………………………...…………Monocyte chemoattractant-1

NIH…………………………..………………………………..Neointimal hyperplasia

ROS………………………………………………………….Reactive oxygen species

PTX…………………………………….....…………………………....Paclitaxel

PTA……………………………………...……….Percutaneous transluminal angioplasty

PAD……………………………………………..……………Peripheral artery disease

PDGF……………………………………………………..Platelet derived growth factor

PEG……………………………………...………………………..Polyethylene glycol

PC………………………………………………………………..Principal component

PCA……………………………………………………….Principal component analysis

RCT…………………………………………….…………Randomized clinical trials

RBC.……………………………………...……………………………Red blood cell

TF……………………………….………………………………………Tissue factor

TNFSRF9/CD137………...………..Tumor necrosis factor receptor superfamily member 9

VSMC…………………………………………………...Vascular smooth muscle cell

INTRODUCTION

Cardiovascular disease

Cardiovascular disease (CVD) is a group of disorders that involve the heart and blood vessels. The main risk factors of CVD include hypertension, obesity, smoking, lack of physical activity, poor diet, and diabetes.[1] Globally, 18.8 million deaths are attributed to CVD, making it the world's first leading cause of death.[1] In the United States, more than 30.3 million people are diagnosed with CVD, resulting in approximately 659,000 deaths each year.[1] Despite the steady decline of CVD mortality rates over the last 40 years, the prevalence of disease risk factors remains high. Many problems of CVD are related to atherosclerosis which is the build-up of plaque in the blood vessels. This leads to the hardening of the vessels called stenosis and narrowing of the vessel lumen, decreasing blood flow. Rupture of the plaque can cause occlusions and clotting of the artery leading to stroke, myocardial infarction, acute coronary syndrome, stable angina, peripheral artery disease, gangrene, and amputation.

Peripheral artery disease

Lower extremity peripheral artery disease (PAD) is the stenosis and occlusion of large arteries in the legs which are often associated with adverse clinical outcomes.[2-4] PAD is the third leading cause of atherosclerotic morbidity after coronary heart disease[2] and affects >230 million people worldwide.[4] The prevalence of PAD in the United States for people >40 years of age is 8.5 million, and the risk increases substantially with age.[4] Although the vast majority of those with PAD do not have symptoms or functional limitations, and many have limited ability to walk and a significantly reduced quality of life.[2-5]

In the early stages of PAD, arteries compensate for the build-up of plaque with vessel dilation.[5] Eventually, the narrowing of the lumen occurs as the vessel is unable to dilate any further, increasing the risk of sudden ischemia and embolisms. Complications in the femoral artery area is the most common, followed by iliac, then popliteal arteries.[5] As the narrowing continues, there is a shift of blood flow to smaller parallel arterial networks to preserve distal perfusion but it does not carry as much blood as the main artery.[5] Patients with PAD reach a point during physical exertion where the collateral blood flow is maximized and cannot provide additional perfusion to lower extremities. The lack of perfusion during these situations manifests as temporary muscle cramps, pain, and fatigue until the energy demands meet the blood supply again.[5] Critical limb ischemia (CLI) is the severe form of PAD as poor perfusion can cause ischemia, presenting with pain at rest, non-healing wounds, and tissue loss.[3-5] Over a 5-year period, it is estimated that 5-10% of asymptomatic PAD patients will develop CLI.[3] The most severe cases of CLI can lead to the development of gangrene and amputation with mortality after five years in approximately 25% of patients.[4,6]

Types of vascular interventions

Endovascular revascularization and surgical interventions are therapies of PAD that intend to alleviate symptoms, preserve limb integrity by increasing blood flow, and increase the quality of life.[1-3,7] Percutaneous transluminal angioplasty (PTA) and stenting are the mainstream techniques used for endovascular revascularization.[7] PTA is the introduction of a deflated balloon catheter through the affected artery. The balloon is then inflated to provide the arterial lumen patency against and flatten the plaque. Additionally, a cylindrical metal mesh called a stent can be permanently inserted to reduce the narrowing of the blood vessel in the future. When the occlusion is not suitable for PTA and stenting, bypass surgeries can be performed to redirect the blood flow.[8] Atherectomy, which is the removal of plaque from the vessel wall, can be done alone or in combination with PTA and stenting.[8]

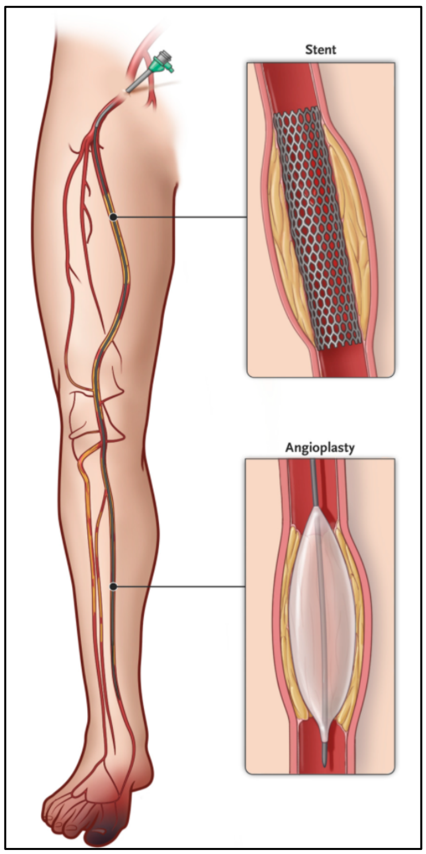

Figure 1. Stent with balloon angioplasty
Graphic representation percutaneous transluminal angioplasty and stenting. Insets demonstrate the placement of a stent in the femoral artery and a balloon angioplasty in the posterior tibial artery.[3]

Balloons

The major drawback with PTA and stenting alone are high rates of restenosis ranging from 30-60% within the first year of operation.[9] Restenosis is the re-narrowing of a vessel at the site it was treated. It is largely attributed to neointimal hyperplasia (NIH), which is the thickening of the tunica intima and involves the proliferation and migration of vascular smooth muscle cells (VSMCs) as a physiological healing response.[10] Drug-coated balloons (DCBs) are angioplasty balloons that deliver a high concentration of an anti-restenotic agent to the inner arterial wall.[7,9] The chosen agent must be highly lipophilic to ensure quick delivery to the vessel and retention for long-term effects. It must also have minimal toxicity to the local vascular wall and in the systemic circulation. In addition, the agent should also be able to provide even distribution to the blood vessel during the application, be stable during transport and handling, and also have a long shelf-life.[11]

Paclitaxel (PTX) is the single most potent anti-restenotic agent tested.[12] PTX binds to the beta subunit of tubulin resulting in disassembly of microtubules and inhibition of cell division.[12] It is highly lipophilic meaning it has a high-fat affinity and it is also hydrophobic, so it does not bind to aqueous media such as blood. PTX is delivered along with an excipient molecule to provide rapid uptake into target vessels.[11] Only four types of DCBs are currently available in the United States: In. Pact Admiral by Medtronic, Lutonix by BD Interventional, Stellarex by Philip, and Ranger by Boston Scientific Corporation.[11,13-15] DCBs mainly differ in the concentration of the drug, nature of the coating, and the excipient.[11]

The In. Pact Admiral DCB has the highest PTX concentration at 3.5 μg/mm^2 between the four DCBs, the rest being at a low dose of 2μg/mm^2.[11] The higher drug concentration of the In. Pact Admiral results in the higher transfer rate of the drug to the target vessel at the cost of greater loss into the systemic circulation and possible distal embolization.[11] Low-dose DCBs are just as effective at providing sufficient drug concentrations for a comparable anti-restenotic effect.[16]

The coating of PTX on the balloon can range from amorphous to crystalline. Amorphous PTX is highly durable during transport and handling to effectively deposit the drug on the targeted vessel. However, studies have shown that drug retention in amorphous PTX is not comparable to crystalline PTX.[17-18] Crystalline PTX is more brittle during transport and handling but is very efficient at depositing the drug in the vessel.[17] The crystalline structure allows for PTX to better dissolve into the tissue and may form reservoirs for sustained drug release.[17] Granada et al.[18] demonstrated in a rabbit study that arterial wall PTX concentrations 1H following balloon inflation were the same between the crystalline and amorphous form. At 24 hour follow-up, crystalline PTX concentrations were constant while amorphous PTX concentration had decreased by 99%.[18]

An excipient helps to maximize PTX adherence during transport and deposition on tissue walls during balloon inflation.[17] Polyethylene glycol (PEG) is a non-toxic, large hydrophilic molecule that forms a plastic-like coating when used with water.[17] This allows for greater adaptability of the balloon during transport-caused deformation, compression, deflation, and final inflation. Urea is another hydrophilic molecule used as an excipient. Once hydrated, both PEG and urea swell and separate PTX molecules from each other, increasing the bioreactivity and absorption into the arterial wall.[17] Polysorbate/sorbitol coating acts as an emulsifier to accelerate PTX dissolution. However, acetyl tributyl citrate is a hydrophobic excipient that aims to balance drug transfer and retention.[17]

Several randomized clinical trials (RCTs) have examined the beneficial effects of DCBs compared to conventional PTA and bare-metal stents in preventing restenosis.[9,19-20]This has set DCBs at the forefront of battling limb loss. Rosenfield et al.[19] conducted an RCT of 476 patients and determined that the primary patency in the first year was higher in the DCB group than in the conventional balloon angioplasty group (65% versus 53%; P=0.02). Another RTC which followed up with patients up to 24 months after the operation, further demonstrated higher primary patency at two years post-operation in the DCB group compared to conventional balloon angioplasty (79% versus 50%; P<0.001).[20] Additionally, a recent meta-analysis study that examined 6 trials with 541 patients found that use of DCB was significantly associated with reduced restenosis at 6 and 12 months.[9]

Stents

There are two types of stents currently in use for PAD, bare metal stents (BMS) and drug-eluting stents (DESs). BMS was the first generation of stents introduced for revascularization therapy in patients with PAD. BMSs are categorized into balloon-expandable stents and self-expandable stents. Balloon-expandable stents are usually made from stainless steel or chromium-cobalt.[21] However, these are not suitable to the deformities that arteries experience during limb flexion and are usually not used for PAD treatment.[21] Self-expandable stents are made from nitinol, an intermetallic compound called nitinol composed of nickel and titanium to exhibit super-elastic and shape memory characteristics suitable for correction of stress-induced deformities.[22] Nitinol is able to expand to a pre-set shape and size once released from the catheter and, more importantly, able to reshape after being deformed during limb flexion.[22] The main disadvantage of BMS is the diffuse in-stent restenosis after its permanent deployment.[7]

DES attempts to reduce the frequency of restenosis caused by NIH with anti-restenotic drugs, the most common being PTX.[6] Currently there are 2 DESs on the US market that differ by PTX dosage and coating profile: Eluvia by Boston Scientific Corporation and Zilver by Cook Ireland Itd.[14] Eluvia is designed with a lower dose of PTX (0.167 μg/mm^2) with a fluoropolymer coating compared to the polymer-free Zilver (3.0 μg/mm^2).[11] The fluoropolymer coating provides a slower drug release by releasing 40% of PTX within the first 30 days of implantation and up to 90% eluted at 12 months.[11] Conversely, polymer-free stents release 95% of PTX within the first 24H and continues to elute over 56 days.[23]

Several RCTs have reported the superior clinical outcomes of DESs compared to BMSs.[6,24-25] A large RCT involving >2300 PAD patients examined the second and third-year clinical outcomes of DES and BMS procedures.[24] At year 3, the clinical end points of restenosis, non-fatal myocardial infarction, and all-cause mortality was lower in the DES group than the BMS group.[24] Dake et al.[25], evaluated the clinical durability between DES and BMS in 236 PAD patients. The study demonstrated >40% of relative reduction in risk of restenosis in the DES group 5-year post-procedure.[25] Similar findings were seen in a recent study of 256 PAD patients, which reported significantly reduced restenotic rates in DES (16%) compared to BMS (35%) after 3-years.[6]

The Potential adverse effect of PXT coated devices

This thesis was motivated by a controversial article published recently. In late 2018, Katsanos et al.[12] conducted a systemic review and meta-analysis of DCB and DES devices in the femoral and/or popliteal arteries. This study analyzed 28 RTCs which included 4663 patients with a primary patency endpoint between 6 -24 months and a maximum follow-up period of up to 5 years.[12] The study examined the all-cause death at 1, 2, and 5-year between PTX coated balloons or stents versus control arms. Evidence demonstrated that all-cause death at 1-year had the same crude risk of 2.3% for both PTX and control arms.[12] However, the crude risk of all-cause death increased dramatically for the PTX arm at year 2 (7.2% vs 3.8%) and year 5 (14.7% vs 8.1%).[12] The authors considered the findings to be of particular concern as PTX mediated devices were under routine clinical use.

The unexpected data effectively resulted in a warning from the FDA and precipitated a drop in the use of PTX mediated devices.[26] The actual mechanism linking PTX devices to mortality remains unknown. Furthermore, this study underscored a need to find another safer yet effective agent to be used alone or alongside PTX in DCBs or DESs to achieve the same therapeutic benefit.

Dexamethasone

Dexamethasone (DEX) is a synthetic glucocorticoid with profound anti-inflammatory and anti-proliferative effects.[27] DEX has been demonstrated to inhibit the function of immune cells and tumor growth.[27] The major effect which DEX acts is through the inhibition of cell-cycle proteins such as platelet-derived growth factor (PDGF) chain A and interleukin-1 beta (IL-1b).[28-29] Inhibition of PDGF and IL-1b have been shown to reduced VSMC migration and proliferation.[29] DEX also inhibits adhesion molecule expression on endothelial cells (ECs) to effectively reduce the number of infiltrating immune cells at the site of vessel injury.[30] DEX has further been shown to decrease collagen synthesis and metalloproteases which play a role in VSMC migration and thus, NIH and restenosis.[29] As PAD is an atherosclerotic disease with the main pathogenicity deriving from inflammation, DEX serves has a promising alternative agent to reduce the risk of restenosis in endovascular revascularization therapy. In vitro studies have demonstrated the ability of DEX to inhibit VSCM migration and proliferation.[27,31] Additionally, several in vivo studies using rat and rabbit models have demonstrated that DEX coated balloons were able to inhibit the proliferation of VSMCs.[30,32] Similar results were seen in a swine model using DEX eluting stents to examine NIH.[33]

PTX is massively released in the systemic circulation after the its application which is the hypothesized problem to induce cardiovascular death. This thesis aims to examine the toxicity of PTX in ECs to shed more light on the higher mortality rates associated with PTX devices and the potential of DEX to abrogate the systemic effects.

METHODS

Cell Culture

Raw pooled donor human umbilical vascular endothelial cells (HUVECs) (Cat No. C2519AS) were obtained from Lonza and grown in EGM-2 media made from EBM-2 media supplemented with EGM-2 bulletkit (Cat No. CC-3162; Lonza). HUVEC-TERT cells were grown in RPMI-1640 media supplemented with 10% FBS and 1% penicillin and streptomycin. Cells were incubated in a 37˚C humidified incubator with 5% CO_2.

Gelatin Coated Tissue Culture Plates

Primary human endothelial cells were grown in gelatin-coated plates. 2 g of type A gelatin powder (Cat No. G1890;Sigma) was added to 100 mL diH_2O and mixed until dissolved. 2% Gelatin solution was autoclaved for 15 mins and cooled down to room temperature before being store at 4˚C. To coat plates, 2% gelatin solution was warmed up in 37˚C water bath. 2 mL of gelatin solution was added to each well in a 6 well plate for 30 secs before removal. Plates were air-dried for at least 1 hour prior to seeding cells.

Drugs

Paclitaxel (Cat No. P9600; LC Laboratories) and dexamethasone (Cat No. 11015; Cayman Chemical Company) were dissolved in dimethyl sulfoxide (Cat No. D8418-250ML; Sigma).

Alamarblue Cell Viability Assay

90 uL of HUVEC cells were seeded in 96 well plates at 5000 cells/well and treated with vehicle, PTX, DEX, or PTX+DEX for 18H. 10 uL of Alamarblue solution (Cat No. Bio-Rad BUF012B) was added to each well and gently mixed with tapping. Cultures were

incubated with the dye for 4H, and spectrophotometry measurements (TECAN M1000) were taken at 570 nm and 600 nm. Cell viability values were calculated using the equation in Figure 2.

$$= \frac{(O2 \times A1) - (O1 \times A2)}{(O2 \times P1) - (O1 \times P2)} \times 100$$

Figure 2. Alamarblue cell viability equation.
O1 = molar extinction coefficient (E) of oxidized alamarBlue (blue) at 570 nm, O2 = E of oxidized alamarBlue at 600 nm, A1 = absorbance of test wells at 570 nm, A2 = absorbance of test wells at 600 nm, P1 = absorbance of positive growth control well (cells plus alamarBlue but no test agent) at 570 nm, P2 = absorbance of positive growth control well (cells plus alamarBlue but no test agent) at 600 nm.

RNA Extraction

HUVEC-TERT cells were seeded in p60 plates and treated with DMSO, PTX, or DEX at ~60% confluence for 24H and harvested for RNA extraction following RNeasy Mini Kit (Cat No. 74104; Qiagen). First the cell medium was aspirated then washed with cold PBS 3 times. 350 µL of RLT buffer was added to lyse cells. Plates were scraped with a rubber scraper, lysate was collected into an RNeasy spin column and 350 µL of 70% ethanol was added. Columns were centrifuged for 30 seconds at 10,000 rpm and flow-through was discarded. To eliminate genomic contamination, on-column DNase digestion was performed using RNase-free DNase set (Cat No. 79254; Qiagen). To wash the spin column, 350 µL RW1 buffer was added and centrifuged for 30 seconds at 10,000 rpm. Flow-through was discarded. 80 µL of DNase I solution was added directly to the center of the spin column membrane and treated for 15 minutes at room temperature (RT). To remove the DNase I solution, the spin column was treated with 350 µL of RW1 buffer, spun at 10,000 rpm for 30 seconds, and the flow-through discarded. The spin column was washed with two treatments of 500 µL RPE buffer and spun for 2 minutes at 10,000 rpm. Longer centrifugation ensures the removal of residual ethanol, which can interfere with downstream processing. RNA was eluted with 40 µL of RNase-free water. RNA concentration was measured with a spectrophotometer (BioDrop).

RNA Sequencing and Analysis

HUVEC-TERT cells were grown in the presence of DMSO control or various concentrations of PTX (5 nM, 50 nM, 500 nM) or DEX (1 µM, 10 µM, 100 µM) and each group was represented in triplicate. The quality of each sample was assessed with FastQC (version 0.11.7) and RSeQC (version 3.0.0). Several sex-specific genes (XIST, DDX3T, KDM5D, RPS4Y1, USP9Y, UTY) were assessed to determine which sex the cell line was derived from. STAR (version 2.6.0c) was used to examine the alignment of each samples to the genome and total reads were tabulated where there was at least one alignment to the mitochondrial chromosome and where there was at least one alignment to the sense or antisense strand of annotated rRNA loci or rRNA repeats. Files were aligned to human genome build hg38. Then total sets of uniquely aligned, properly paired reads were tabulated and separated as: assigned to single Ensembl gene locus, not assigned to any Ensembl gene loci, or assigned to more than one Ensembl gene locus (ambiguous). Ensembl-gene-level counts were generated with featureCounts (version 1.6.2), and Ensembl annotation build 100.

Principal component analysis (PCA) was then performed which is a mathematical transformation that collapses the variance between samples with a large set of variables into a smaller set of variables called principal components (PC). This was done using the DESeq2 R package (version 1.23.10). PC1 explains the most variance in the data, followed by PC2, etc. PCA was done first across all genes and all samples and then computed between DMSO vs. PTX group and DMSO vs. DEX group. Differential expression analysis was done with a one-way analysis of variance (ANOVA) to identify genes whose expression changes were with respect to the treatment. Benjamini-Hochberg False Discovery Rate (FDR) correction was applied to obtain FDR-corrected p values. This represents the probability that a given result is a false positive based on the overall distribution of p values. Two-way ANOVA was done to identify genes whose expression changed with respect to agent, dose, or interaction of the two. To obtain a test statistic and p values for each gene using pairwise comparison, the Wald test was conducted.

Genes were subsequently clustered based on expression filters which analyzes treatment effect across all groups and treatment effect within PTX and DEX groups. Heatmaps were generated using clustering analysis with z-scores ranging between ≤ -2, 0, ≥ 2 represented by blue, white, and red, respectively.

Gene set enrichment analysis (GSEA) (version 2.2.1) identified sets of genes that were up- or down-regulated with respective to a given comparison. All genes were ranked with Wald statistic and pairwise comparison with gene sets obtained from the Molecular Signatures Database (version 7.4). A significant GSEA value for a gene set suggests that the pathway or process is relevant to the experimental comparison.

Western Blot

HUVEC-TERT cells in p60s were harvested after 48H drug treatment. Cell media was first aspirated then washed with cold PBS three times. 120 µL of RIPA buffer was added to each plate and plates were scraped with a rubber cell scraper to detach and lyse cells; samples were collected into an Eppendorf tube on ice. Samples were frozen and thawed with liquid nitrogen and 37˚C water bath three times and centrifuged for 10 mins at 14,000 rpm and 4˚C to ensure sufficient cell lysis and collection of cell pellet. Bradford assay and measurement with a spectrophotometer were used to quantify and standardize protein concentration. Samples were prepared in 4X dye with 8% β-mercaptoethanol, heated at 95˚C for 5 mins. Proteins were separated with 15% SDS–polyacrylamide gel electrophoresis at 100V for 93 mins in 1X running buffer with and transferred to a nitrocellulose membrane at 100V for 45 mins in 1X transfer buffer with 20% methanol. Quality of protein transfer was examined with ponceau s stain (Cat No. P7170; Sigma) and 5% non-fat milk solution was used for protein blocking for 1H at room temperature. Membranes were incubated in primary antibodies diluted with 0.05% sodium azide , 1% BSA in TBST solution for 48H at 4˚C followed by three washes in TBST for 20 mins each. Information about antibodies and their dilutions can be found in Table 1. Secondary antibody (Cat No. 1706515; BioRad) was diluted in 1% non-fat milk and incubated for 1 hour at room temperature, followed by three washes in TBST for 5 mins each. Proteins were visualized with chemiluminescent substrate (Cat No. 34577; Thermo Scientific) and developing machine (Evolve).

Table 1: Primary antibodies used for western blot

Primary Antibody	Vendor	Catalog Number	Dilution
CKS-2	Abcam	ab155078	1:100
BMF	Cell Signaling	50542S	1:100
CD137	Cell Signaling	34594S	1:100
MCP-1	Cell Signaling	81559S	1:100
HSP90	Cell Signaling	8165S	1:1000

Migration Assay and Imaging

HUVEC cells were grown in 6 well plates until 60% confluency and treated with drugs for 18H. A single scratch with a P1000 pipette tip was induced on the monolayer. Media was aspirated and 2 ml of new drug-treated media was added after scratch. Baseline, immediately after scratch, 6H, 24H, 48H post scratch images were taken.

Image processing

All images were taken with Nikon Eclipse Ti inverted microscope with bright field camera at the Boston University School of Medicine (BUSM) Imaging Core (https://www.bumc.bu.edu/ cellular-imaging/). NIS-Elements software was the platform used for controlling the microscope and documenting photos. 6 fields of 10X images were taken randomly with phase 1 lenses to create a wide-field image. X, Y and Z coordinates of the scratch in each well were saved onto the microscopy software so that each time point would have the image at the same location to reduce variability. Images were exported as full-resolution tagged image file format (TIF) and quantified with Image J software. The "straight line" tool was used to make a random horizontal straight line across the scratch to measure the distance of the gap on three different locations of the same sample. Each sample was repeated in triplicate. The distance of the gap was taken at a random location for the same well at different time points. The straight line was then added to the "ROI manager" and values were measured in pixels.

Statistical analysis

Parameters were expressed as mean, median, standard deviation, and standard error of the mean (SEM). A comparison of groups was performed using independent student's t-tests where p value less than 0.05 was considered significant. In selected cases, adjustments were performed for multiple comparison using Bonferroni correction. A regression analysis was used using linear regression. All the p values less than 0.05 were deemed significant as statistical analyses were performed using excel and Prism software.

RESULTS

Paclitaxel negatively regulates fundamental endothelial functions

The inhibitory role of PTX in the cell viability was confirmed with Alamarblue assay in HUVECs. Alamarblue is a resazurin-based blue dye that uses the reducing power of living cells to change into resofurin, a red coloured dye. Cells were split into 96 well plates and treated with DMSO control, PTX, or DEX for 18H prior to the addition of Alamarblue dye. Readings at 570 nm and 600 nm were taken after 4H of incubation. Results showed that cell viability reduced in a dose-dependent manner with PTX reaching half-maximal inhibitory concentration (IC50) at 0.05μM (Figure 3A). To examine the potential of DEX to increase cell viability on PTX-mediated devices, ECs were treated with DEX and PTX together. 10μM of DEX was able to increase cell viability in the group treated with 5nM PTX but had no effect in the group treated with 50nM PTX (Figure 3B-3C). Compared to the PTX only group, the addition of DEX was able to significantly increase cell viability (Figure 3D). These results suggest that PTX significantly suppresses EC viability and proliferation and DEX is able to partially rescue PTX-treated EC functions.

Dexamethasone does not induce migration in paclitaxel treated endothelial cells

A migration assay was used to examine the migratory effects of endothelial cells when treated with PTX and DEX. Triplicates of HUVEC cells were treated with DMSO, PTX, DEX, or PTX + DEX in 6 well plates for 18 hours where a scratch on the monolayer was applied. There was a marginal increase of EC migration with DEX treatment compared to control, 70% vs 63% respectively ($p=0.05$). At 24H, the ECs have migrated to completely cover the scar in the control and DEX-only groups. In contrast, there was no change in scar length in the PTX and PTX+DEX groups through 48H (Figure 4A-4B). However, DEX does not have any detrimental effects on the induced scar of PTX treated cells. This demonstrates that although DEX is not able to rescue scar formation of PTX treated ECs, it does not further implicate the damage.

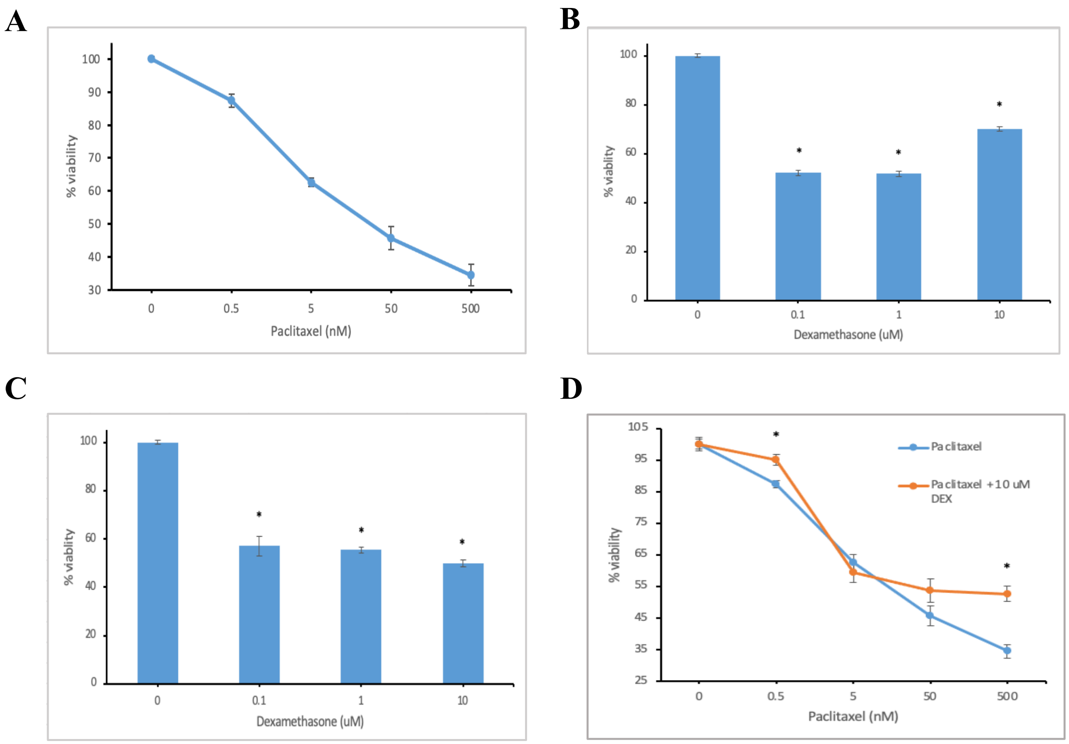

Figure 3. Effects of paclitaxel and dexamethasone on endothelial cell viability. (A) HUVECs were treated with 0, 0.5, 5, 50, 500nM paclitaxel (PTX) for 18H. (B) HUVEC viability with 0.5 nM PTX and 0, 0.1, 1, or 10µM dexamethasone (DEX) for 18H. (C) HUVEC viability with 5 nM PTX and 0, 0.1, 1, or 10µM DEX for 18H. (D) HUVEC viability treated with 10µM DEX and 0, 0.5, 5, 50, 500 nM PTX for 18H. Blue line represents PTX only group and orange line represents PTX and 10 uM DEX group. HUVECs were treated with drugs and Alamarblue dye was added at 10% of total volume after 18H. Readings at 570nm and 600 nm were taken after 4H incubation. Error bars = SEM. (n=6). **P* < 0.05 versus no treatment HUVECs. 0, control; DMSO control.

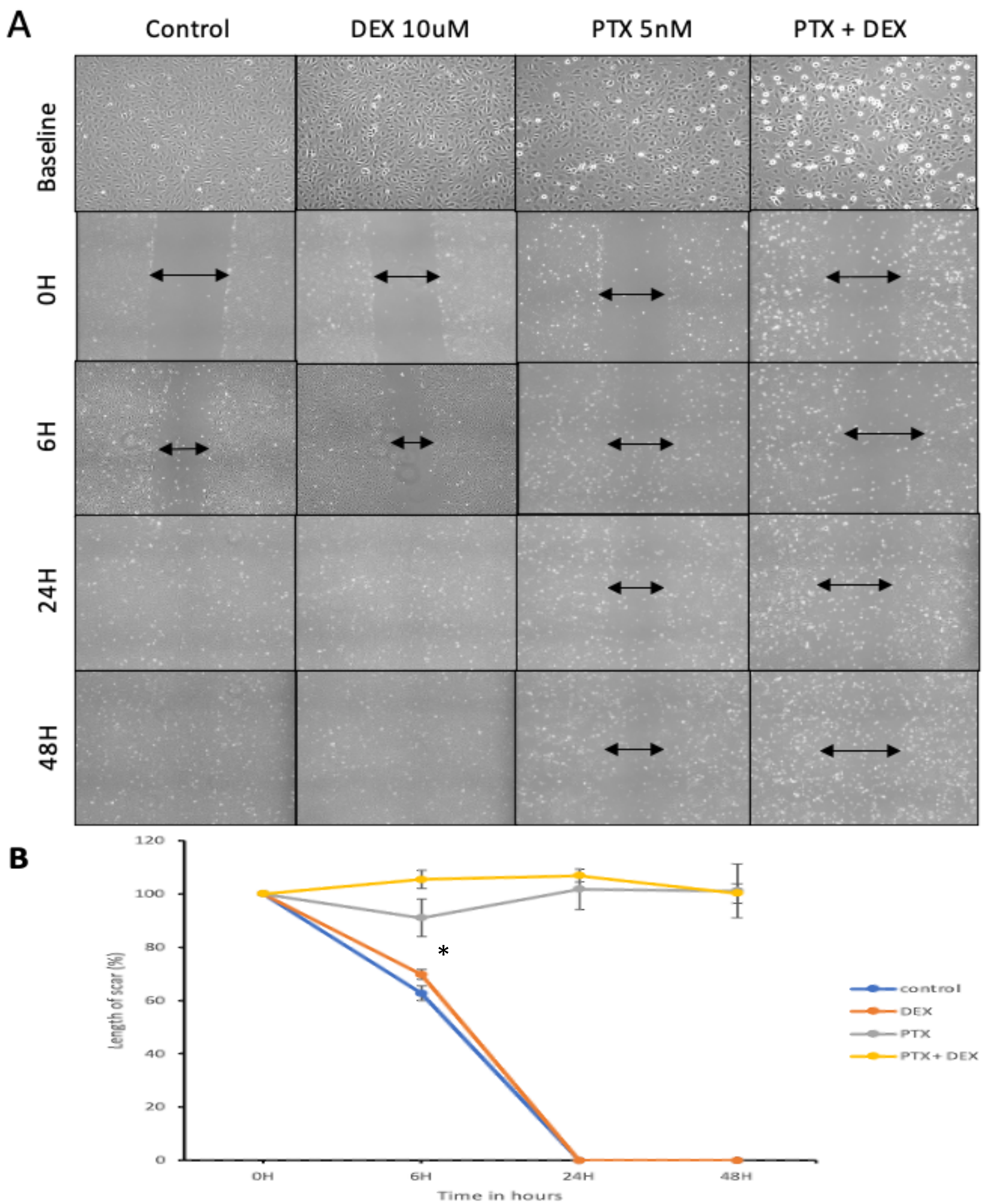

Figure 4. Endothelial cell migration assay. (A) Migration assay over 48H. HUVECs were treated with control, 10µM dexamethasone (DEX), 5nM paclitaxel (PTX), or 10µM DEX and 5nM PTX. 10X images were taken of each experimental arm at baseline, immediately after scratch, 6, 24 and 48H post scratch. Images were taken at the same location at each time point. (B) Endothelial migration with control, DEX, PTX, and PTX+DEX treatment. Length of scratch (pixels) was randomly taken using Image J and length at 0H was used as 100% to create a percentage value for each time point. Error bars = SEM. **P* = 0.05 versus control HUVECs; DMSO control.

Paclitaxel modulates a wide array of genetic programs in endothelial cells

To understand how PTX modulates ECs, RNA sequencing was performed on samples extracted from HUVEC-TERTs in control arm, and treated with PTX, or DEX for 24H. Overall, approximately 30,000,000 genes were examined between control and drug-treated groups which aligned to the reference genome. Clustering analysis was done for all treatment groups to separate functionally close gene-sets into groups. The result was 6 different clusters, 3 of which had the greatest number of differentially expressed genes between each group (Figure 5A-5D). The results revealed agent-dependent changes in gene expression, and thus, each gene was examined at transcriptional levels. Expression of monocyte chemoattractant-1 (MCP-1), tumor necrosis factor receptor superfamily member 9 (TNFSRF9/CD137), CDC28 protein kinase regulatory subunit-2 (CKS-2), and Bcl2 modifying factor (BMF) were found to be inversely affected in PTX, and DEX treated groups. A 2-fold increase in transcription levels of MCP-1 was observed with PTX treatment compared to a 1.8-fold decrease with DEX treatment. Similarly, transcription levels of CD137 and CKS-2 also increased in the PTX group (1.3-fold and 2-fold) and decreased in the DEX group (1.2-fold for both). In contrast, BMF had a 1.5-fold decrease with PTX and a 1.3-fold increase with DEX. The results demonstrate differentially expressed genes modulated by PTX and DEX, which can be leveraged for therapeutic purposes.

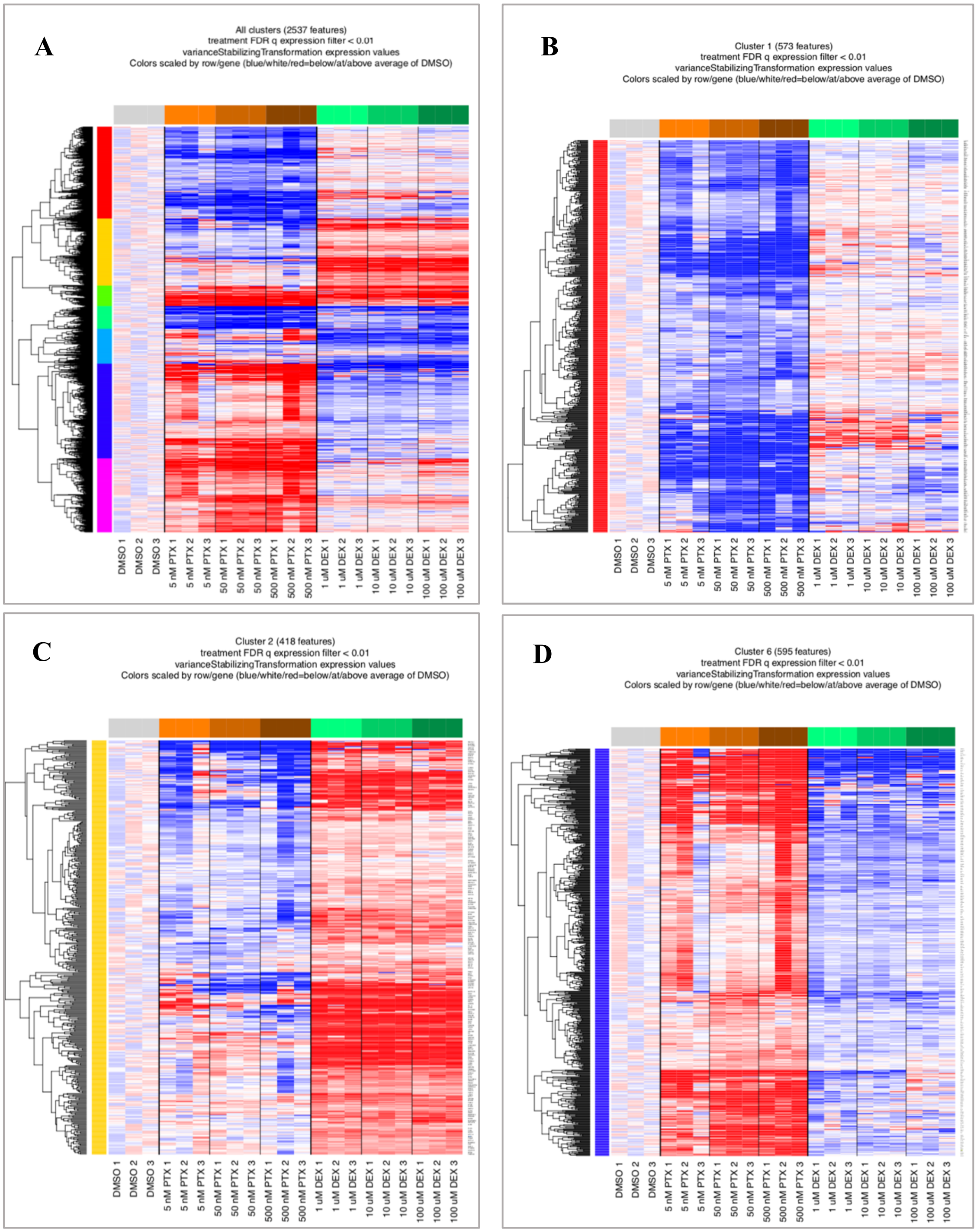

Figure 5. Heatmap representation of differentially expressed genes between PTX and DEX-treated ECs. (A) Heatmap for expression of all genes of DMSO vs PTX vs DEX treated ECs. (B) Characterization of genes in cluster 1 of DMSO vs PTX vs DEX treated ECs. (C) Characterization of genes in cluster 2 of DMSO vs PTX vs DEX treated ECs. (D) Characterization of genes in cluster 6 of DMSO vs PTX vs DEX treated ECs. Colours are scaled by row and gene (blue/white/red = below/at/above average of DMSO).

Dexamethasone has a protective effect against genes modulated by paclitaxel in endothelial cells

Changes in RNA expression may not always be representative of protein synthesis. For this reason, western blot analysis was performed to validate the effects of PTX and DEX on differentially expressed levels of MCP-1, CD137, CKS-2, and BMF (Figure 6A-6D). HUVEC-TERT cells were seeded in p60 plates and treated with control, PTX, or DEX for 48H prior to harvest. Protein expression of targeted genes was consistent with RNA-sequencing data. MCP-1, CD137, and CKS-2 increased with PTX and decreased with DEX, while BMF decreased with PTX and increased with DEX. Cells were treated with 1µM and 10µM of DEX in the presence of 5nM PTX to investigate the differences in protein expression. It was revealed that DEX was able to down-regulate protein expression of MCP-1, CD137, and CKS-2 in the presence of 5nM of PTX (Figure 7B-7D). Furthermore, BMF levels were maintained by DEX despite the addition of PTX (Figure 7A). Collectively, this data suggests the potential of DEX to partially abrogate the toxicity of PTX in endothelial cells.

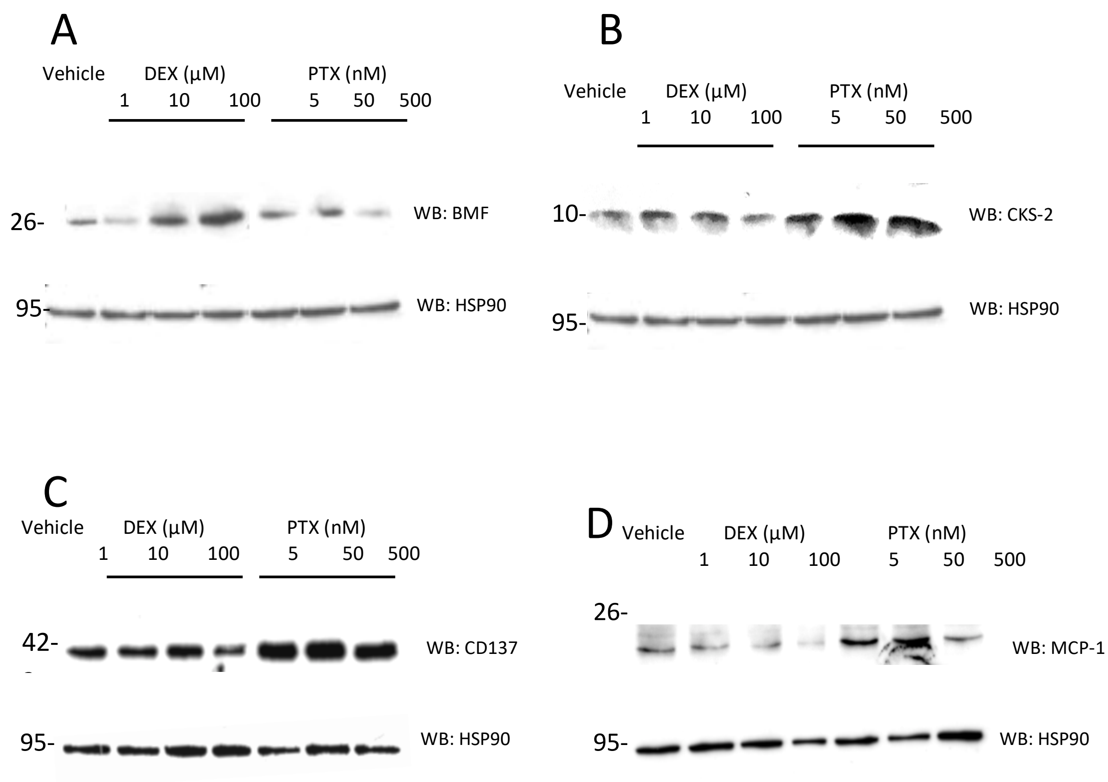

Figure 6. Differentially expressed proteins by PTX and DEX treated ECs.
(A) HUVEC-TERTs were treated with DMSO, PTX or DEX for 48H at indicated concentrations to probe for BMF. (B) HUVEC-TERTs were treated with DMSO, PTX or DEX for 48H at indicated concentrations to probe for CKS-2. (C) HUVEC-TERTs were treated with DMSO, PTX or DEX for 48H at indicated concentrations to probe for CD137. (D) HUVEC-TERTs were treated with DMSO, PTX or DEX for 48H at indicated concentrations to probe for MCP-1. HSP90 served as loading control.

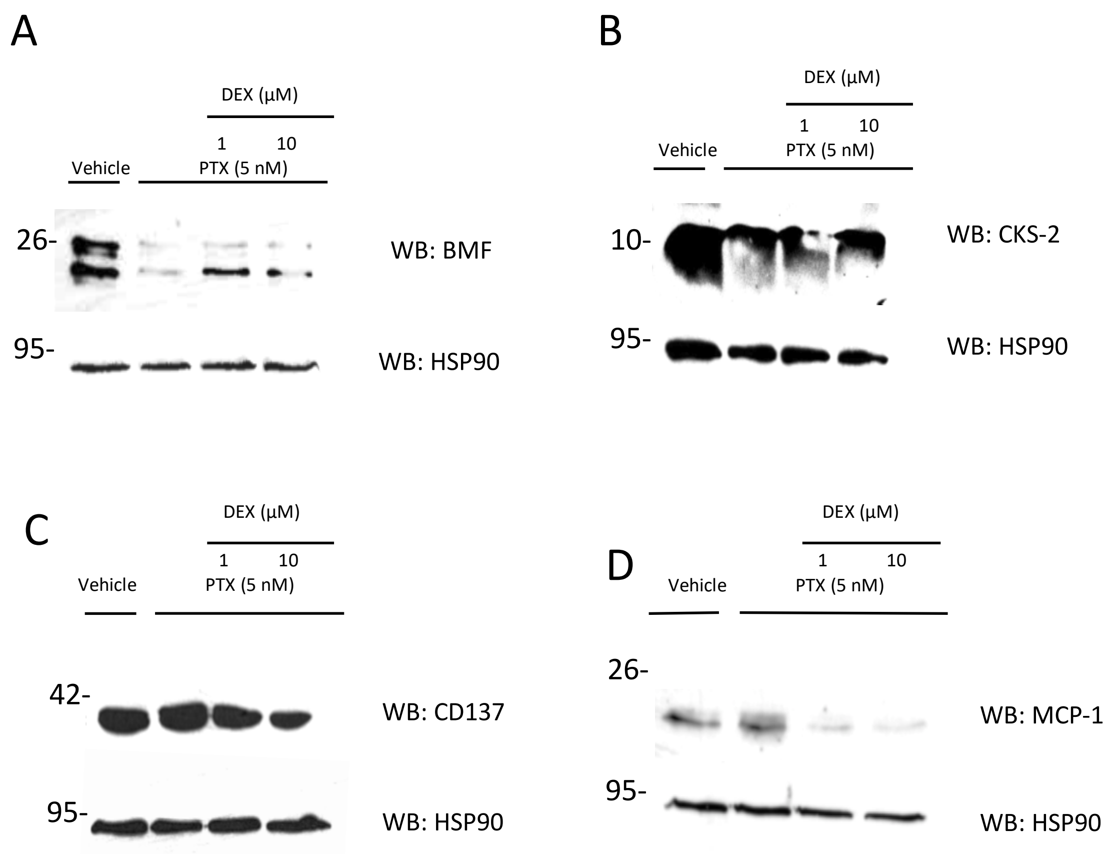

Figure 7. DEX has protective function in proteins modulated by PTX. HUVEC-TERTs were treated with vehicle control (DMSO), 5nM PTX, and 1μM or 10μM DEX for 48H. Cells were probed with western blot (A) BMF, (B) CKS-2, (C) CD137, (D) MCP-1. HSP90 served as loading control.

DISCUSSION

This line of investigation was inspired by the by Katsanos et al.study [12] which showed increased mortality in patients treated with paclitaxel-coated balloons. Our hypothesis is that acute exposure to PTX induces changes in distant endothelial cells, which may accelerate CVD and a potential increase in CV events as reported by Katsanos et al.[12] We set out to understand the mechanisms of PTX induced perturbations in ECs. For that, we used fundamental biological functions of ECs and RNA sequencing analysis to emulate the use of balloon application in humans.

PTX enforces its anti-proliferative effect by binding to β-tubulin and disrupting the microtubule dynamic during cell division. This event inhibits the proliferation of VSMC and hence, it was effective in reducing NIH following angioplasty and restenotic lesions. However, PTX has no differential effect on endothelial cells. PTX inhibits endothelial cell proliferation in the reactive vascular bed after balloon or stent injury. Such endothelial wounds remain open exposing highly thrombogenic subendothelial matrix and VSMCs. This phenomenon may account for subacute or chronic stent thrombosis observed with drug-eluting stents. Although these are local complications as noted above, Katsanos et al.[12] showed increased mortality in patients treated with PTX eluting balloons and stents raising a possibility of more systemic and delayed effects. This notion was emulated with in vitro models. It has been shown that application of PTX-coated balloon results in deposition of a large quantity of PTX in the vessel wall,[18] higher than its IC50 of 0.67μM, which can account for potent inhibition of endothelial cells and VMSCs. However, the balloon application is also followed by increased blood levels of PTX, primarily coming from the PTX which was washed away with blood after the balloon deflates. This massive spike in PTX may induce systemic toxicity.

To explore the above hypothesis, the experimental design consisted of exposing cells to various concentrations of PTX and DEX. The differential regulation of genes showed that there were several genes that changed with PTX in a dose-dependent manner. From the array of genes that were modulated by PTX, we then focused on genes that were regulated by DEX in an opposite manner i.e. those genes upregulated by PTX and downregulated by DEX or vice versa. Amongst them, we found BMF, CKS-2, CD137, and MCP-1 and were validated by western blot analysis (Figure 5-6).

BMF is an pro-apoptotic factor[34] that was downregulated by PTX and upregulated by DEX in a dose-dependent manner. BMF binds to prosurvival protein Bcl-2 to induce cell death.[35] Our study demonstrated that BMF was upregulated by DEX and downregulated by PTX. CKS-2 interacts with cyclin-dependent kinases to play critical roles in cell cycle regulation and may be involved as a promoter of tumor progression.[36] Karra et al.[37] examined human gene sets showed that CKS-2 was associated with the development of atherosclerosis. The mechanism(s) by which CKS-2 augment atherosclerotic progression remains unclear.[37] Our study showed that PTX upregulated and concurrent use of DEX downregulated CKS-2 in ECs by PTX.

CD137 is best known for its co-stimulatory function in T lymphocyte activation for immune response. Its expression is also found in ECs.[38] The amplified CD137 signalling in ECs leads to endothelial dysfunction which subsequently increases the expression of adhesion molecules and pro-inflammatory cytokines. This increases the recruitment and migration of leukocytes to exacerbate the progression of atherosclerosis.[38-40] CD137 was also found to be upregulated in ECs by PTX and downregulated by DEX. MCP-1 is a potent chemokine upregulated by paclitaxel and downregulated by DEX. For this study, we focused on MCP-1 due to its involvement in the pathogenesis of atherosclerosis.

MCP-1 or CCL2 is a monomeric polypeptide that weighs 9-15 kDa; it is one of the key chemokines belonging to the CC family which regulate migration and recruitment of monocytes.[41] MCP-1 also exerts various pro-inflammatory effects on monocytes such as cytokine production, adhesion molecule expression, and induction of reactive oxygen species (ROS) release.[41,42] Chemokines have 3 domains: (1) high flexible N-terminal domain, (2) long loop that leads into three anti-parallel β-pleated sheets, and (3) α-helix overlying the sheets.[41] MCP-1 binds to the transmembrane receptor C-C chemokine receptor type 2 (CCR2), forming dimers to activate G-protein coupled receptors.[41] MCP-1 has been demonstrated to play an important role in the development of NIH.[42]

Egashira et al.[42] demonstrated that persistent activation of MCP-1 resulted in pro-longed vascular inflammation, upregulation of cytokines and chemokines, and proliferation of VSMCs. To examine the presence of monocytes and VSMCs during vascular injury, a mouse model with mutant MCP-1 was used to compare with wild-type MCP-1 mice.[42] The investigators found a lack of monocyte infiltration and VSMC proliferation in mice with mutant MCP-1.[42] Additionally, a clinical study observed that plasma MCP-1 levels were higher in patients who developed restenosis after PTA compared to non-restenotic patients after PTA.[43] This further supports the potential involvement of MCP-1 in the development of restenosis in patients that undergo endovascular therapies.

High MCP-1 levels have been detected in atherosclerotic lesions compared to normal arteries, suggesting the involvement of MCP-1 in the development of atherosclerosis.[43] MCP-1 interacts with monocytes by binding to CCR2, resulting in diapedesis into the subendothelial layer.[44] Once in the tissue, macrophages enhance the inflammatory response by secreting inflammatory mediators such as cytokines and chemokines and other growth factors. Activated monocytes/macrophages also promote additional recruitment of and infiltration of monocytes to the site of inflammation. As inflammation proceeds, macrophages engulf low-density lipoproteins and become foam cells. Eventually, foam cells collect and result in the formation of fatty streaks.[45] Using genetically altered rodent models, several studies demonstrated the importance of MCP-1 in the development of atheromatous lesions.[44-46] Boring et al.[46] showed that deletion of CCR2 dramatically reduced the formation of diet-induced atherosclerotic lesions. Furthermore, lesion formation was also inhibited in mice with mutant MCP-1 and CCR2.[45,46]

Inflammation is a known determinant of plaque instability and rupture of an atherosclerotic plaque is associated with thrombotic events with potentially life-threatening complications. There are several mechanisms that contribute to the development of a vulnerable plaque including increased neovascularity and increased cap matrix breakdown.[47] MCP-1 has been demonstrated to in involved in both of these processes.[45] Enlargement of the plaque and the thickening of the intima results in local ischemia and this triggers angiogenesis in the affected vessel.[48] Neovascularization in atherosclerosis is the disorganized growth of blood vessels in the atherosclerotic plaque.[49] The immature capillaries may lead to leakage of red blood cells (RBCs) and the influx of oxygen and nutrients, promoting plaque progression.[48,49] The presence of excess RBCs results in intraplaque hemorrhage, providing a source of erythrocyte-derived phospholipids to serve as an alternate cholesterol substrate.[50] The rapid change in plaque substrate may promote a transition from stable plaque to unstable plaque.[50] Several studies have demonstrated the proangiogenic effects of MCP-1 and its association with plaque vulnerability through animal models.[45,51-54]

MCP-1 also plays a role in the disruption of atherosclerotic plaques by inducing matrix metalloproteinases (MMP).[45] MMPs allow leukocytes to permeate the EC barrier and into the subendothelial layer by degrading collagens and other structural proteins.[45,55] As inflammation continues, high levels of MCP-1 lead to continual degradation and thinning of the atherosclerotic cap, thus increasing the risk of plaque rupture.[55] In addition, MCP-1 is capable of upregulating tissue factor (TF) synthesis, further contributing to the prothrombotic and life-threatening complications of atherosclerotic lesions.[45]

Our study has demonstrated the ability of DEX to suppress the effects of MCP-1 in endothelial cells. RNA sequencing of HUVEC-TERTs demonstrated a 1.8-fold decrease in MCP-1 transcription levels when treated with DEX compared to control and PTX. This was validated with protein analysis where protein expression of MCP-1 was suppressed when ECs were treated with DEX compared to control and PTX groups. HUVEC-TERTs treated with 5nM of PTX were also treated with 1μM or 10μM of DEX to examine the expression of MCP-1. We found that DEX had a dose-dependent response suppression of MCP-1. The inhibition of MCP-1 by DEX may have also contributed to the marginal increase of EC migration across a wound compared to control.

Limitations and future studies

The limitations of this study lie in the use of only HUVECs. The use of different types of endothelial cell lines such as human primary coronary artery endothelial cells or renal glomerular endothelial cells would have allowed for a more comprehensive view of PTX induced toxicity in the systemic circulation. Using a 3D cell culture model would have also better recapitulated EC migration over a wound inflicted by a balloon or stent. Additionally, one can use single-cell sequencing to have a detailed analysis of PTX toxicity. This study also does not directly link PTX/DEX induced modulation of MCP-1, CKS-2, CD137, and BMF to endothelial damage or death. Perhaps some staining, gene silencing experiments or cell apoptosis assays could be done to analyze the relationship. Finally, in vivo studies such as the use of a murine model would help to further understand and validate the pathogenic mechanisms of PTX. Murine models would also be used to evaluate the potential of DEX as an alternative anti-restenotic agent.

Conclusion

In conclusion, this work for the first time examines potential mediators of PTX-induced systemic toxicity emanating from spike in the levels of PTX observed after PTX-coated balloon treatment. This event may trigger systemic effects enhancing atherothrombotic events. We hope that this study paves the way for future analysis to understand the mechanisms and mediators of PTX-induced systemic toxicity and adverse cardiovascular events in humans and the means to abrogate it.

REFERENCES

1. Virani, S. S., Alonso, A., Aparicio, H. J., Benjamin, E. J., Bittencourt, M. S., Callaway, C. W., Carson, A. P., Chamberlain, A. M., Cheng, S., Delling, F. N., Elkind, M. S. V., Evenson, K. R., Ferguson, J. F., Gupta, D. K., Khan, S. S., Kissela, B. M., Knutson, K. L., Lee, C. D., Lewis, T. T., & Liu, J. (2021). Heart Disease and Stroke Statistics—2021 Update: A Report From the American Heart Association. *Circulation*, *143*(8). https://doi.org/10.1161/cir.0000000000000950

2. Shu, J., & Santulli, G. (2018). Update on peripheral artery disease: Epidemiology and evidence-based facts. *Atherosclerosis*, *275*, 379–381. https://doi.org/10.1016/j.atherosclerosis.2018.05.033

3. Farber, A. (2018). Chronic Limb-Threatening Ischemia. *New England Journal of Medicine*, *379*(2), 171–180. https://doi.org/10.1056/nejmcp1709326

4. Criqui, M. H., Matsushita, K., Aboyans, V., Hess, C. N., Hicks, C. W., Kwan, T. W., McDermott, M. M., Misra, S., & Ujueta, F. (2021). Lower Extremity Peripheral Artery Disease: Contemporary Epidemiology, Management Gaps, and Future Directions: A Scientific Statement From the American Heart Association. *Circulation*, *144*(9). https://doi.org/10.1161/cir.0000000000001005

5. Zemaitis, M. R., Fatmata Bah, Boll, J. M., & Dreyer, M. A. (2019, June 28). *Peripheral Arterial Disease*. Nih.gov; StatPearls Publishing. https://www.ncbi.nlm.nih.gov/books/NBK430745/

6. Falkowski, A., Bogacki, H., & Szemitko, M. (2020). Assessment of Mortality and Factors Affecting Outcome of Use of Paclitaxel-Coated Stents and Bare Metal Stents in Femoropopliteal PAD. *Journal of Clinical Medicine*, *9*(7), 2221. https://doi.org/10.3390/jcm9072221

7. Hiramoto, J. S., Teraa, M., de Borst, G. J., & Conte, M. S. (2018). Interventions for lower extremity peripheral artery disease. *Nature Reviews Cardiology*, *15*(6), 332–350. https://doi.org/10.1038/s41569-018-0005-0

8. Robertson, L., Paraskevas, K. I., & Stewart, M. (2017). Angioplasty and stenting for peripheral arterial disease of the lower limbs: an overview of Cochrane Reviews. *Cochrane Database of Systematic Reviews*. https://doi.org/10.1002/14651858.cd012542

9. Cao, S., He, T., Xie, J., Feng, H., Liu, K., Qu, B., & Wu, X. (2021). Drug-coated balloon angioplasty versus balloon angioplasty for treating patients with in-stent restenosis in the femoropopliteal artery: A meta-analysis. *Medicine*, *100*(16), e25599. https://doi.org/10.1097/MD.0000000000025599

10. Kruger, D. (2012). Neo-intimal hyperplasia, diabetes and endovascular injury : review article. *Cardiovascular Journal of Africa*, *23*(9), 507–511. https://doi.org/10.5830/cvja-2012-019

11. Lindquist, J., & Schramm, K. (2018). Drug-Eluting Balloons and Drug-Eluting Stents in the Treatment of Peripheral Vascular Disease. *Seminars in Interventional Radiology*, *35*(5), 443–452. https://doi.org/10.1055/s-0038-1676360

12. Katsanos, K., Spiliopoulos, S., Kitrou, P., Krokidis, M., & Karnabatidis, D. (2018). Risk of Death Following Application of Paclitaxel-Coated Balloons and Stents in the Femoropopliteal Artery of the Leg: A Systematic Review and Meta-Analysis of Randomized Controlled Trials. *Journal of the American Heart Association*, *7*(24). https://doi.org/10.1161/jaha.118.011245

13. Fornell, D. (2021, March 16). *Overview of Angioplasty Balloon Technology Advances*. DAIC. https://www.dicardiology.com/article/overview-angioplasty-balloon-technology-advances

14. Health, C. for D. and R. (2021). Paclitaxel-Coated Balloons and Stents for Peripheral Arterial Disease. *FDA*. https://www.fda.gov/medical-devices/cardiovascular-devices/paclitaxel-coated-balloons-and-stents-peripheral-arterial-disease

15. http://fyra.io. (n.d.). *Drug-Coated Balloons (SFA/Popliteal Indication)*. Endovascular Today. Retrieved February 15, 2022, from https://evtoday.com/device-guide/us/drug-coated-balloons

16. Liistro, F., & Di Mario, C. (2020). Paclitaxel-coated balloons in peripheral artery disease: how much is enough? *European Heart Journal*, *41*(27), 2553–2555. https://doi.org/10.1093/eurheartj/ehaa239

17. Ramachandran, M., & Owens, M. S. (2017). (2017). The Stellarex Difference: Critical Components of an Optimal DCB. *Supplement and Endovascular Today*, *16*(9).https://assets.bmctoday.net/evtoday/pdfs/et0917_Spectranetics_Supp_sec%202.pdf

18. Granada, J. F., Stenoien, M., Buszman, P. P., Tellez, A., Langanki, D., Kaluza, G. L., Leon, M. B., Gray, W., Jaff, M. R., & Schwartz, R. S. (2014). Mechanisms of tissue uptake and retention of paclitaxel-coated balloons: impact on neointimal proliferation and healing. *Open Heart*, *1*(1), e000117. https://doi.org/10.1136/openhrt-2014-000117

19. Rosenfield, K., Jaff, M. R., White, C. J., Rocha-Singh, K., Mena-Hurtado, C., Metzger, D. C., Brodmann, M., Pilger, E., Zeller, T., Krishnan, P., Gammon, R., Müller-Hülsbeck, S., Nehler, M. R., Benenati, J. F., Scheinert, D., & LEVANT 2 Investigators. (2015). Trial of a Paclitaxel-Coated Balloon for Femoropopliteal

Artery Disease. *The New England Journal of Medicine*, *373*(2), 145–153. https://doi.org/10.1056/NEJMoa1406235

20. Laird, J. R., Schneider, P. A., Tepe, G., Brodmann, M., Zeller, T., Metzger, C., Krishnan, P., Scheinert, D., Micari, A., Cohen, D. J., Wang, H., Hasenbank, M. S., Jaff, M. R., & IN.PACT SFA Trial Investigators. (2015). Durability of Treatment Effect Using a Drug-Coated Balloon for Femoropopliteal Lesions: 24-Month Results of IN.PACT SFA. *Journal of the American College of Cardiology*, *66*(21), 2329–2338. https://doi.org/10.1016/j.jacc.2015.09.063

21. Maleckis, K., Anttila, E., Aylward, P., Poulson, W., Desyatova, A., MacTaggart, J., & Kamenskiy, A. (2018). Nitinol Stents in the Femoropopliteal Artery: A Mechanical Perspective on Material, Design, and Performance. *Annals of Biomedical Engineering*, *46*(5), 684–704. https://doi.org/10.1007/s10439-018-1990-1

22. Stoeckel, D., Pelton, A., & Duerig, T. (2004). Self-expanding nitinol stents: material and design considerations. *European Radiology*, *14*(2), 292–301. https://doi.org/10.1007/s00330-003-2022-5

23. Dake, M. D., Van Alstine, W. G., Zhou, Q., & Ragheb, A. O. (2011). Polymer-free paclitaxel-coated Zilver PTX Stents--evaluation of pharmacokinetics and comparative safety in porcine arteries. *Journal of Vascular and Interventional Radiology: JVIR*, *22*(5), 603–610. https://doi.org/10.1016/j.jvir.2010.12.027

24. Applegate, R. J., Sacrinty, M. T., Kutcher, M. A., Santos, R. M., Gandhi, S. K., & Little, W. C. (2009). 3-Year Comparison of Drug-Eluting Versus Bare-Metal Stents. *JACC: Cardiovascular Interventions*, *2*(3), 231–239. https://doi.org/10.1016/j.jcin.2008.12.010

25. Dake, M. D., Ansel, G. M., Jaff, M. R., Ohki, T., Saxon, R. R., Smouse, H. B., Machan, L. S., Snyder, S. A., O'Leary, E. E., Ragheb, A. O., & Zeller, T. (2016). Durable Clinical Effectiveness With Paclitaxel-Eluting Stents in the Femoropopliteal Artery. *Circulation*, *133*(15), 1472–1483. https://doi.org/10.1161/CIRCULATIONAHA.115.016900

26. Beckman, J. A., & White, C. J. (2019). Paclitaxel-Coated Balloons and Eluting Stents: Is There a Mortality Risk in Patients With Peripheral Artery Disease? *Circulation*, *140*(16), 1342–1351. https://doi.org/10.1161/circulationaha.119.041099

27. Reil, T. D., Sarkar, R., Kashyap, V. S., Sarkar, M., & Gelabert, H. A. (1999). Dexamethasone Suppresses Vascular Smooth Muscle Cell Proliferation. *Journal of Surgical Research*, *85*(1), 109–114. https://doi.org/10.1006/jsre.1999.5665

28. Radke, P. W., Weber, C., Kaiser, A., Schober, A., & Hoffmann, R. (n.d.). Dexamethasone and Restenosis After Coronary Stent Implantation: New Indication for an Old Drug? *Current Pharmaceutical Design*, *10*(4), 349–355. Retrieved February 15, 2022, from https://www.eurekaselect.com/article/7535
29. Xu, W., Guo, T., Zhang, Y., Jiang, X., Zhang, Y., Zen, K., Yu, B., & Zhang, C.-Y. (2011). The inhibitory effect of dexamethasone on platelet-derived growth factor-induced vascular smooth muscle cell migration through up-regulating PGC-1α expression. *Experimental Cell Research*, *317*(8), 1083–1092. https://doi.org/10.1016/j.yexcr.2010.10.006

30. Villa, A. E., Guzman, L. A., Chen, W., Golomb, G., Levy, R. J., & Topol, E. J. (1994). Local delivery of dexamethasone for prevention of neointimal proliferation in a rat model of balloon angioplasty. *Journal of Clinical Investigation*, *93*(3), 1243–1249. https://doi.org/10.1172/jci117078

31. Pross, C., Farooq, M. M., Angle, N., Lane, J. S., Cerveira, J. J., Xavier, A. E., Freischlag, J. A., Law, R. E., & Gelabert, H. A. (2002). Dexamethasone Inhibits Vascular Smooth Muscle Cell Migration via Modulation of Matrix Metalloproteinase Activity. *Journal of Surgical Research*, *102*(2), 57–62. https://doi.org/10.1006/jsre.2001.6220

32. Petrik, P. V., Law, M. M., Moore, W. S., Colburn, M. D., Quiñones-Baldrich, W., & Gelabert, H. A. (1998). Dexamethasone and enalapril suppress intimal hyperplasia individually but have no synergistic effect. *Annals of Vascular Surgery*, *12*(3), 216–220. https://doi.org/10.1007/s100169900143

33. Seo, T.-S., Oh, J.-H., Park, Y.-K., Song, H.-Y., Park, S. J., & Yuk, S.-H. (2005). Efficacy of a Dexamethasone-Eluting Nitinol Stent on the Inhibition of Pseudointimal Hyperplasia in a Transjugular Intrahepatic Portosystemic Shunt: An Experimental Study in a Swine Model. *Korean Journal of Radiology*, *6*(4), 241. https://doi.org/10.3348/kjr.2005.6.4.241

34. Piñon, J. D., Labi, V., Egle, A., & Villunger, A. (2008). Bim and Bmf in tissue homeostasis and malignant disease. *Oncogene*, *27*(1), S41–S52. https://doi.org/10.1038/onc.2009.42

35. Labi, V., Erlacher, M., Kiessling, S., Manzl, C., Frenzel, A., O'Reilly, L., Strasser, A., & Villunger, A. (2008). Loss of the BH3-only protein Bmf impairs B cell homeostasis and accelerates γ irradiation–induced thymic lymphoma development. *Journal of Experimental Medicine*, *205*(3), 641–655. https://doi.org/10.1084/jem.20071658

36. Huang, N., Wu, Z., Hong, H., Wang, X., Yang, F., & Li, H. (2019). Overexpression of CKS2 is associated with a poor prognosis and promotes cell proliferation and

invasion in breast cancer. *Molecular Medicine Reports*. https://doi.org/10.3892/mmr.2019.10134

37. Karra, R., Vemullapalli, S., Dong, C., Herderick, E. E., Song, X., Slosek, K., Nevins, J. R., West, M., Goldschmidt-Clermont, P. J., & Seo, D. (2005). Molecular evidence for arterial repair in atherosclerosis. *Proceedings of the National Academy of Sciences*, *102*(46), 16789–16794. https://doi.org/10.1073/pnas.0507718102

38. Yuan, W., Xu, C., Li, B., Xia, H., Pan, Y., Zhong, W., Xu, L., Chen, R., & Wang, B. (2021). Contributions of Costimulatory Molecule CD137 in Endothelial Cells. *Journal of the American Heart Association*, *10*(11). https://doi.org/10.1161/jaha.120.020721

39. Olofsson, P. S., SöderströmL. Å., WågsäterD., Sheikine, Y., Ocaya, P., LangF., Rabu, C., Chen, L., Rudling, M., AukrustP., Hedin, U., Paulsson-Berne, G., SirsjöA., & HanssonG. K. (2008). CD137 Is Expressed in Human Atherosclerosis and Promotes Development of Plaque Inflammation in Hypercholesterolemic Mice. *Circulation*, *117*(10), 1292–1301. https://doi.org/10.1161/circulationaha.107.699173

40. Jung, I.-H., & Oh, G. T. (2016). The Roles of CD137 Signaling in Atherosclerosis. *Korean Circulation Journal*, *46*(6), 753–761. https://doi.org/10.4070/kcj.2016.46.6.753

41. Deshmane, S. L., Kremlev, S., Amini, S., & Sawaya, B. E. (2009). Monocyte Chemoattractant Protein-1 (MCP-1): An Overview. *Journal of Interferon & Cytokine Research*, *29*(6), 313–326. https://doi.org/10.1089/jir.2008.0027

42. Egashira, K., Zhao, Q., Kataoka, C., Ohtani, K., Usui, M., Charo, I. F., Nishida, K., Inoue, S., Katoh, M., Ichiki, T., & Takeshita, A. (2002). Importance of Monocyte Chemoattractant Protein-1 Pathway in Neointimal Hyperplasia After Periarterial Injury in Mice and Monkeys. *Circulation Research*, *90*(11), 1167–1172. https://doi.org/10.1161/01.res.0000020561.03244.7e

43. Cipollone, F., Marini, M., Fazia, M., Pini, B., Iezzi, A., Reale, M., Paloscia, L., Materazzo, G., D'Annunzio, E., Conti, P., Chiarelli, F., Cuccurullo, F., & Mezzetti, A. (2001). Elevated circulating levels of monocyte chemoattractant protein-1 in patients with restenosis after coronary angioplasty. *Arteriosclerosis, Thrombosis, and Vascular Biology*, *21*(3), 327–334. https://doi.org/10.1161/01.atv.21.3.327

44. Zhang, X., Liu, X., Shang, H., Xu, Y., & Qian, M. (2011). Monocyte chemoattractant protein-1 induces endothelial cell apoptosis in vitro through a p53-

dependent mitochondrial pathway. *Acta Biochimica et Biophysica Sinica*, *43*(10), 787–795. https://doi.org/10.1093/abbs/gmr072

45. Gonzalez-Quesada, C., & Frangogiannis, N. G. (2009). Monocyte Chemoattractant Protein (MCP-1)/CCL2 as a biomarker in Acute Coronary Syndromes. *Current Atherosclerosis Reports*, *11*(2), 131–138. https://www.ncbi.nlm.nih.gov/pmc/articles/PMC2787514/

46. Boring, L., Gosling, J., Cleary, M., & Charo, I. F. (1998). Decreased lesion formation in CCR2−/− mice reveals a role for chemokines in the initiation of atherosclerosis. *Nature*, *394*(6696), 894–897. https://doi.org/10.1038/29788

47. Shah, P. K. (2003). Mechanisms of plaque vulnerability and rupture. *Journal of the American College of Cardiology*, *41*(4), S15–S22. https://doi.org/10.1016/s0735-1097(02)02834-6

48. Jaipersad, A. S., Lip, G. Y. H., Silverman, S., & Shantsila, E. (2014). The Role of Monocytes in Angiogenesis and Atherosclerosis. *Journal of the American College of Cardiology*, *63*(1), 1–11. https://doi.org/10.1016/j.jacc.2013.09.019

49. Camaré, C., Pucelle, M., Nègre-Salvayre, A., & Salvayre, R. (2017). Angiogenesis in the atherosclerotic plaque. *Redox Biology*, *12*, 18–34. https://doi.org/10.1016/j.redox.2017.01.007

50. Virmani, R., Kolodgie, F. D., Burke, A. P., Finn, A. V., Gold, H. K., Tulenko, T. N., Wrenn, S. P., & Narula, J. (2005). Atherosclerotic Plaque Progression and Vulnerability to Rupture. *Arteriosclerosis, Thrombosis, and Vascular Biology*, *25*(10), 2054–2061. https://doi.org/10.1161/01.atv.0000178991.71605.18

51. Salcedo, R., Ponce, M. L., Young, H. A., Wasserman, K., Ward, J. M., Kleinman, H. K., Oppenheim, J. J., & Murphy, W. J. (2000). Human endothelial cells express CCR2 and respond to MCP-1: direct role of MCP-1 in angiogenesis and tumor progression. *Blood*, *96*(1), 34–40. https://doi.org/10.1182/blood.V96.1.34

52. Qiu, J., Lei, D., Hu, J., Yin, T., Zhang, K., Yu, D., & Wang, G. (2017). Effect of intraplaque angiogenesis to atherosclerotic rupture-prone plaque induced by high shear stress in rabbit model. *Regenerative Biomaterials*, *4*(4), 215–222. https://doi.org/10.1093/rb/rbx007

53. Georgakis, M. K., van der Laan, S. W., Asare, Y., Mekke, J. M., Haitjema, S., Schoneveld, A. H., de Jager, S. C. A., Nurmohamed, N. S., Kroon, J., Stroes, E. S. G., de Kleijn, D. P. V., de Borst, G. J., Maegdefessel, L., Soehnlein, O., Pasterkamp, G., & Dichgans, M. (2021). Monocyte-Chemoattractant Protein-1 Levels in Human Atherosclerotic Lesions Associate With Plaque Vulnerability. *Arteriosclerosis,*

Thrombosis, and Vascular Biology, *41*(6), 2038–2048. https://doi.org/10.1161/atvbaha.121.316091

54. Liu, X. L., Zhang, P. F., Ding, S. F., Wang, Y., Zhang, M., Zhao, Y. X., Ni, M., & Zhang, Y. (2012). Local Gene Silencing of Monocyte Chemoattractant Protein-1 Prevents Vulnerable Plaque Disruption in Apolipoprotein E-Knockout Mice. *PLoS ONE*, *7*(3), e33497. https://doi.org/10.1371/journal.pone.0033497

55. Robinson, Stephen C., Scott, Kate A., & Balkwill, Frances R. (2002). Chemokine stimulation of monocyte matrix metalloproteinase-9 requires endogenous TNF-α. *European Journal of Immunology*, *32*(2), 404–412. https://doi.org/3.0.co;2-x">10.1002/1521-4141(200202)32:2<404::aid-immu404>3.0.co;2-x

CURRICULUM VITAE

[redacted]

[redacted]

[redacted]

[redacted]